Available online at www.sciencedirect.com
ScienceDirect
Vision Research 47 (2007) 2751–2766
Vision Research
www.elsevier.com/locate/visres

Wave aberrations in rhesus monkeys with vision-induced ametropias ☆

Ramkumar Ramamirtham [a,b], Chea-su Kee [a,1], Li-Fang Hung [a,b], Ying Qiao-Grider [a,b], Juan Huang [a,b], Austin Roorda [a,2], Earl L. Smith III [a,b,*]

[a] College of Optometry, University of Houston, 505 J Davis Armistead Building, Houston, TX 77204-2020, USA
[b] Vision CRC, Sydney, NSW 2052, Australia

Received 10 April 2007; received in revised form 24 July 2007

Abstract

The purpose of this study was to investigate the relationship between refractive errors and high-order aberrations in infant rhesus monkeys. Specifically, we compared the monochromatic wave aberrations measured with a Shack–Hartman wavefront sensor between normal monkeys and monkeys with vision-induced refractive errors. Shortly after birth, both normal monkeys and treated monkeys reared with optically induced defocus or form deprivation showed a decrease in the magnitude of high-order aberrations with age. However, the decrease in aberrations was typically smaller in the treated animals. Thus, at the end of the lens-rearing period, higher than normal amounts of aberrations were observed in treated eyes, both hyperopic and myopic eyes and treated eyes that developed astigmatism, but not spherical ametropias. The total RMS wavefront error increased with the degree of spherical refractive error, but was not correlated with the degree of astigmatism. Both myopic and hyperopic treated eyes showed elevated amounts of coma and trefoil and the degree of trefoil increased with the degree of spherical ametropia. Myopic eyes also exhibited a much higher prevalence of positive spherical aberration than normal or treated hyperopic eyes. Following the onset of unrestricted vision, the amount of high-order aberrations decreased in the treated monkeys that also recovered from the experimentally induced refractive errors. Our results demonstrate that high-order aberrations are influenced by visual experience in young primates and that the increase in high-order aberrations in our treated monkeys appears to be an optical byproduct of the vision-induced alterations in ocular growth that underlie changes in refractive error. The results from our study suggest that the higher amounts of wave aberrations observed in ametropic humans are likely to be a consequence, rather than a cause, of abnormal refractive development.

Keywords: Refractive error; High-order aberrations; Myopia; Hyperopia; Astigmatism

1. Introduction

High-order, monochromatic, wavefront aberrations are caused primarily by optical imperfections such as surface irregularities and tilts or misalignments in the eye's optical components and like traditional spherical and astigmatic refractive errors these high-order aberrations can significantly influence retinal image quality (Campbell & Gubisch, 1966; Howland & Howland, 1976; Jenkins, 1963; Liang, Grimm, Goelz, & Bille, 1994; Liang & Williams, 1997; Smirnov, 1961). Virtually all eyes exhibit high-order aberrations and although the pattern and magnitude of high-order aberrations vary substantially between individuals (Carkeet, Luo, Tong, Saw, & Tan, 2002; Caste-

☆ Supported by National Eye Institute Grants RO1 EY03611 and P30 EY07551 and funds from the Vision CRC, Sydney Australia and the Greeman-Petty Professorship, UH Foundation.
* Corresponding author. Address: College of Optometry, University of Houston, 505 J Davis Armistead Building, Houston, TX 77204-2020, USA. Fax: +1 713 743 0965.
E-mail address: esmith@uh.edu (E.L. Smith III).
[1] Present address: School of Optometry, The Hong Kong Polytechnic University, Hong Kong, SAR, China.
[2] Present address: School of Optometry, University of California at Berkeley, Berkeley, CA, USA.

0042-6989/$ - see front matter © 2007 Elsevier Ltd. All rights reserved.
doi:10.1016/j.visres.2007.07.014

jon-Mochon, Lopez-Gil, Benito, & Artal, 2002; De Brabander et al., 2004; He, Burns, & Marcos, 2000; He et al., 2002; Porter, Guirao, Cox, & Williams, 2001; Thibos, Hong, Bradley, & Cheng, 2002b), several observations suggest that there is a link between traditional refractive errors and high-order aberrations (Collins, Wildsoet, & Atchison, 1995; He et al., 2002; Llorente, Barbero, Cano, Dorronsoro, & Marcos, 2004; Paquin, Hamam, & Simonet, 2002). For example, it has been reported that myopic humans (Collins et al., 1995; He et al., 2002; Llorente et al., 2004; Paquin et al., 2002), like chickens with experimentally induced myopia (Coletta, Marcos, Wildsoet, & Troilo, 2003; Garcia de la Cera, Rodriguez, & Marcos, 2006; Howland, Tong, Yoko, & Toshifumi, 2004; Kisilak, Campbell, Hunter, Irving, & Huang, 2006), have higher amounts of wavefront aberrations than emmetropes (however, see Carkeet et al., 2002; Cheng, Bradley, Hong, & Thibos, 2003; Legras, Chateau, & Charman, 2004; Porter et al., 2001) and that human myopes show different patterns of aberrations than emmetropes (He et al., 2002; Paquin et al., 2002; Radhakrishnan, Pardhan, Calver & O'Leary, 2004). In addition, shortly after birth normal infant chicks and monkeys exhibit high amounts of wavefront aberrations that decrease systematically during development in a manner that approximately parallels the emmetropization process (Garcia de la Cera et al., 2006; Kisilak et al., 2006; Ramamirtham et al., 2006).

A number of hypotheses have been put forward to explain the association between refractive errors and high-order aberrations. Since emmetropization is an actively regulated vision-dependent process, aberration-induced alterations in retinal image quality could directly affect refractive development in several ways. For example, it is well established that chronic retinal image degradation promotes axial myopia in humans and commonly used laboratory animals (Norton, 1999; Smith, 1998a; Wallman & Winawer, 2004; Wildsoet, 1997). Although the retinal image degradation due to high-order aberrations is usually modest, the degree of high-order aberrations (however, not necessarily the pattern of aberrations) (Cheng et al., 2004; Thibos, 2002) is relatively constant over time, which is critical for a myopigenic stimulus to produce axial elongation (Kee et al., 2007; Napper et al., 1997; Schmid & Wildsoet, 1996; Winawer & Wallman, 2002). Consequently, chronic blur due to aberrations could potentially promote axial myopia (Collins et al., 1995; He et al., 2002; Paquin et al., 2002). It has also been argued that high-order aberrations could alter the end point or reduce the precision of the emmetropization process. Specifically, high amounts of aberrations could effectively increase the depth of focus for the emmetropization process resulting in greater variability and/or by interacting with the eye's refractive error alter the axial position within the 3-D point spread function that is targeted by the emmetropization process (Charman, 2005). Moreover, if the eye uses sign-of-defocus information derived from monochromatic aberrations, which psychophysical studies suggest is possible (Wilson, Decker, & Roorda, 2002), certain patterns or magnitudes of aberrations could mask this sign information and consequently reduce the effectiveness or efficiency of emmetropization resulting in anomalous refractive errors.

An association between refractive errors and aberrations could also come about because ametropic growth alters the normal shape and organization of the eye's optical components. The vision-dependent mechanisms responsible for emmetropization largely exert their influence on vitreous chamber growth (Norton & Siegwart, 1995; Smith, 1998a; Wallman & Winawer, 2004; Wildsoet, 1997). However, alterations in corneal curvature, in particular in corneal toricity, and the aberration structure of the crystalline lens have been documented in eyes with experimentally induced refractive errors (Kee, Hung, Qiao-Grider, Roorda, & Smith, 2004; Kroger, Campbell, & Fernald, 2001; Priolo, Sivak, Kuszak, & Irving, 2000). These results demonstrate that visual experience can produce shape and organizational changes that could alter the eye's high-order aberrations. It is possible that these are passive changes that come about as a consequence of axial and equatorial diameter changes in the globe associated with the local retinal mechanisms that dominate emmetropization. Asymmetrical posterior chamber growth could indirectly via mechanical forces affect corneal shape and/or the geometry and position of the crystalline lens and therefore the eye's aberrations.

In a young adult eye, the aberrations produced by the anterior corneal surface are counterbalanced by aberrations associated with the internal optics of the eye resulting in lower overall aberrations (Artal, Benito, & Tabernero, 2006; Artal, Guirao, Berrio, & Williams, 2001; Atchison, 2004; Kelly, Mihashi, & Howland, 2004; Salmon & Thibos, 2002). For some high-order aberrations, the sign and magnitude of the corneal and internal aberrations appeared to be scaled for each individual, which suggests that some aberrations are influenced by an active developmental process that operates to reduce the eye's total aberrations. In other words, the possibility exists that there are vision-dependent mechanisms that fine tune the compensation between the aberrations produced by the anterior cornea and the eye's internal optics (Artal et al., 2006; Kelly et al., 2004). If that is the case, the ability of these mechanisms to operate could be compromised by the optical defocus associated with an uncorrected refractive error or the visual conditions that lead to anomalous refractive development. Thus, the optical consequences of a refractive error could promote the development of higher than normal amounts of aberrations.

Studies in laboratory animals have provided some insights into the relationship between refractive errors and aberrations. In particular, it has been consistently demonstrated that viewing conditions that promote myopic growth in young chickens, both form deprivation and optically imposed hyperopic defocus, also promote the development of larger amounts of aberrations (Garcia de la Cera et al., 2006; Howland et al., 2004; Kisilak et al.,

2006). Similarly form-deprived marmosets exhibit higher than normal wavefront errors (Coletta, Triolo, Moskowitz, Nickla, & Marcos, 2004). The overall pattern of results suggests that high-order aberrations and the associated reduced in-focus image quality are a consequence rather than a cause of myopia. However, there are currently disagreements concerning whether the higher aberrations in myopic eyes come about primarily as a result of geometrical changes in the eye secondary to excessive axial growth or whether viewing conditions associated with the induced refractive errors interfered with a vision-dependent process that normally optimizes the eye's aberrations (Kisilak et al., 2006).

The purpose of this study was to investigate the relationship between refractive errors and high-order aberrations in infant rhesus monkeys. Specifically, we compared the magnitude and the pattern of wave aberrations between normal monkeys and the monkeys with visually induced refractive errors. We used rhesus monkeys in these experiments because the magnitude and nature of aberrations in rhesus monkey eyes and the structural and optical development of the monkey eye are very similar to those of humans (Bradley, Fernandes, Lynn, Tigges, & Boothe, 1999; Qiao-Grider, Hung, Kee, Ramamirtham, & Smith III, 2007; Ramamirtham et al., 2006). In order to get a broad perspective on the relationship between refractive errors and high-order aberrations, we studied animals with experimentally induced hyperopia, myopia, or astigmatism and monkeys that were recovering from experimentally induced refractive errors.

2. Materials and methods

2.1. Subjects

Our subjects were 64 infant rhesus monkeys (*Macaca mulatta*) obtained at 2–3 weeks of age. All of the rearing and experimental procedures, many of which have been described previously (Hung, Crawford, & Smith, 1995; Smith & Hung, 1999), were approved by the University of Houston's Institutional Animal Care and Use Committee and were in compliance with the National Institutes of Health Guide for the Care and Use of Laboratory Animals.

Normal longitudinal changes in refractive error and the eye's axial dimensions were determined for 26 infants that were reared with unrestricted vision (Hung et al., 1995; Smith, 1998b; Smith, Kee, Ramamirtham, Qiao-Grider, & Hung, 2005). The normal longitudinal changes in the monochromatic ocular aberrations that took place during emmetropization were determined for 8 of these 26 control infants. The initial aberration measures for these control animals were obtained for both eyes at about 3 weeks of age and subsequently at 2- to 4-week intervals for about the first year of life. The aberration data for some of the animals in the control group have been previously reported (Ramamirtham et al., 2006). The effects of altered visual experience on monochromatic wave aberrations were determined for 38 monkeys that were employed in other experiments on the temporal integration properties of the emmetropization process and on the effects of optically imposed defocus or form deprivation on refractive development (Kee et al., 2007; Qiao-Grider, Hung, Kee, Ramamirtham, & Smith, 2002; Smith et al., 2005). The experimental rearing procedures for these monkeys were started at 2–4 weeks of age. All the treated animals wore helmets that held either powered spectacle lenses (-4.5 D, $n = 2$; -3.0 D, $n = 14$; or $+3.0$ D, $n = 10$) or diffuser lenses ($n = 12$) that selectively deprived the periphery of form vision in front of both eyes. The duration of the lens-rearing period varied between 14 and 21 weeks (mean = 121 ± 14 days) and encompassed the rapid early phase of ocular growth and emmetropization, which in normal infant monkeys is largely complete by about 150 days of age (Bradley et al., 1999; Hung et al., 1995; Qiao-Grider et al., 2007). Although the treated subjects represent heterogeneous group, all the visual manipulations were bilateral and optically induced. In part, because the nature and degree of altered visual experience differed between monkeys, our rearing strategies resulted in a wide range of spherical and astigmatic refractive errors. Thus, it was possible to examine the changes in the wave aberrations in monkeys that developed moderate to high levels of myopia and hyperopia.

Systematic longitudinal data on refractive error, monochromatic wave aberrations and axial dimensions were obtained for 31 of the experimental monkeys. For these monkeys, the initial measures were obtained prior to the start of the treatment period and continued until either the end of the rearing period (about 150 days of age, $n = 5$) or until the monkeys were about 300 days of age ($n = 26$). For the remaining 7 treated monkeys, aberration measurements were obtained only twice, specifically, at 2-week intervals between 113 and 170 days of age, i.e., near the end of the lens-rearing period.

2.2. Ocular biometric measurements

The cornea was anesthetized with 1–2 drops of 0.5% tetracaine hydrochloride. Cycloplegia was achieved by topically instilling 2–3 drops of 1% tropicamide 20–30 min before performing any measurement that would potentially be affected by the level of accommodation. To make the necessary measurements each animal was anesthetized with an intramuscular injection of ketamine hydrochloride (15–20 mg/kg) and acepromazine maleate (0.15–0.2 mg/kg). In mice and rats, some anesthetics (e.g., ketamine and xylazine) produce transient cataracts and the loss of a functional tear film, which can produce alterations in wavefront aberrations (Calderone, Grimes, & Shalev, 1986; de la Cera et al., 2006). We have used ketamine-acepromazine anesthesia in all our previous experiments on refractive development and have not observed any alterations in lens clarity in either infant or adult monkeys. However, loss of an intact tear film occurs, presumably because normal blinks are suppressed. Therefore, we used a custom made speculum to gently hold the eyelids apart and the corneal tear film was maintained by frequent irrigation using a saline solution. There were no qualitative differences in the clarity of the spot patterns obtained from our monkeys versus those obtained from awake, fixating humans with the same instrument and, as in humans, the aberration measurements in infant and adolescent monkey eyes were highly repeatable (Ramamirtham et al., 2006). Thus, we believe that any effects of anesthesia on our aberration measurements were negligible.

The refractive status for each eye, which was specified as the spherical-equivalent, spectacle-plane refractive correction, was assessed independently by two experienced investigators using a streak retinoscope and handheld lenses. The mean of these two measurements, specified in minus cylinder form, was taken as an eye's refractive error (Harris, 1988). The eyes' axial dimensions were measured by A-scan ultrasonography implemented with either a 7 (Image 2000; Mentor, Norwell, MA) or 12 MHz transducer (OTI Scan 1000; OTI Ophthalmic Technologies Inc., Ontario Canada). For each eye, ten separate measurements were averaged and the intraocular distances were calculated using velocities of 1532, 1641, and 1532 m/s for the aqueous, lens, and vitreous, respectively. The A-scan measurements were performed after all refractive and aberration measurements were completed.

A custom-built Shack–Hartmann wavefront sensor (SHWS), which was based on the principles described by Liang and Williams (Liang & Williams, 1997; Liang et al., 1994), was used to measure each eye's wave aberrations. For a detailed description of the instrument and the procedures for obtaining aberration measurements in rhesus monkeys see Ramamirtham et al. (2006). Briefly, a low intensity infrared superluminescent diode (10 μW, Hamamatsu Corp., USA) with a wavelength of 830 nm was used to produce a small round spot on the retina. A lenslet array

(Adaptive Optics Associates, Cambridge, MA) composed of a square grid of 0.4 mm-diameter lenslets each with 24 mm focal lengths was used to focus the light emerging from the eye onto a CCD camera. The emerging wavefront was reconstructed from the deviation of the individual spots captured on the CCD camera relative to the spots produced by an ideal planar wavefront. For details on the clarity of the spot pattern and the short- and long-term repeatability of our aberration measurements see Ramamirtham et al. (2006).

The line of sight, which is the recommended reference axis for aberration measurements, passes through the eye's entrance pupil center and connects the fovea to the fixation point (Thibos, Applegate, Schwiegerling, & Webb, 2002a). In monkeys, the line of sight intersects the anterior corneal surface approximately 0.3 mm nasal to the pupillary axis (Quick & Boothe, 1989, 1992). In order to obtain SHWS measurements along the presumed line of sight, each animal was placed on a stage with a head mount that allowed five degrees of movement (X–Y–Z + tip-tilt) to control the animal's pupil location and direction of gaze. The animal's position on the stage was adjusted so that the corneal light reflex produced by the superluminescent diode was 0.3 mm nasal to the pupillary axis thereby ensuring that measured aberrations were referenced to the presumed line of sight. During the course of the measurements, proper alignment was maintained by continuously monitoring the position of the corneal light reflex and the entrance pupil with a video camera.

The refractive error of the eye was not optically corrected, so that both low and high-order aberrations could be measured using the Shack–Hartmann wavefront sensor. Five Shack–Hartmann spot images were obtained for each eye during each session. The images were stored in a computer using a frame grabber and were later analyzed individually using custom software (developed on Microsoft Visual C++ platform) to calculate the relative x–y displacement of each sampled point with respect to the reference center for a given lenslet. This provided the local slopes of the wavefront, which were fit with the derivative of Zernike's circle polynomials (up to 10th order) by the method of least squares. The wave aberration function $W(x,y)$ was represented by a weighted sum of the series of Zernike terms:

$$W(x,y) = \sum_{n,f} C_n^f Z_n^f,$$

where $W(x,y)$ is defined over the x–y coordinates of the pupil, C is the corresponding coefficient of the Zernike term Z, n and f are the degree of the polynomial and the meridional frequency, respectively. We used the double-index convention for naming and ordering the Zernike coefficients and centered the wavefront with the entrance pupil as recommended by the OSA/VSIA Standards Taskforce (Thibos et al., 2002a). Using the average Zernike coefficients obtained from the analysis of 5 such wavefront sensor images, the magnitude of an eye's monochromatic high-order aberrations (3rd and higher order terms), excluding defocus and astigmatism (i.e., 2nd or low order aberrations), was expressed as the total root-mean-square error (RMS) between the measured and ideal wavefronts in units of microns. In addition, the monochromatic point spread function (PSF) and Strehl ratio were calculated from each eye's wavefront aberration function and employed to describe image quality (Charman, 1991; Howland & Howland, 1977; Mahajan, 1991; Walsh & Charman, 1985). All of the spot pattern images were analyzed with a fixed central 5 mm pupil size unless otherwise mentioned. Two treated eyes whose dilated pupil diameter size was less than 5 mm were excluded.

2.3. Statistical analyses

One-tailed, two-sample t-tests were used to determine if the mean aberrations for the animals in the treated group were greater than those for the control group. Pearson's correlation and linear regression analyses were performed to characterize the variations in aberrations as a function of the magnitude of ametropia. Comparisons across subgroups were performed using one-way analyses of variance (ANOVA). If the one-way ANOVA revealed a significant effect, Tukey's pairwise comparisons were used to determine which subgroups were significantly different from the normal control group. The Kruskal–Wallis test was used to determine if the differences in the median aberrations between subject groups were significant. All statistical analyses were performed using Minitab software (ver. 12.21; Minitab Inc., State College, PA).

3. Results

At ages corresponding to the start and end of the lens-rearing period, there were no significant interocular differences in the total RMS wavefront errors, RMS coma, RMS trefoil, or in the amounts of spherical aberration in either the control or experimental subject groups (paired t-test P values = .08–.95). In addition there were no significant interocular differences in spherical-equivalent refractive error or vitreous chamber depth (paired t-test, P values = .25–.67). Therefore, between group statistical comparisons are reported for the right eyes only.

3.1. Refractive error and axial dimensions in control and treated monkeys

At 3 weeks of age, prior to the onset of any experimental treatment, the eyes of the control and the treated monkeys were moderately hyperopic (right eyes, control = +4.10 ± 1.21 D, treated monkeys = +3.94 ± 1.70 D), and there were no between group differences in spherical-equivalent refractive error or vitreous chamber depth (right eyes, two-sample t-test, $P = .79$ for refractive error, $P = .35$ for vitreous chamber depth). In addition, there were no significant differences in the mean total RMS wavefront errors between the treated and the control monkeys, which were 0.46 ± 0.16 μm and 0.50 ± 0.10 μm for the right eyes, respectively (two-sample t-test, $P = .35$).

Over time, the two eyes of each control monkey grew in a coordinated manner toward a low degree of hyperopia, the optimal optical state for young monkeys (Bradley et al., 1999; Hung et al., 1995; Smith & Hung, 1999). The distribution of spherical-equivalent refractive errors for the control monkeys at ages corresponding to the end of treatment period for the experimental monkeys (137 ± 17 days) is shown in Fig. 1a. The distribution was narrowly peaked around a mean of +2.39 ± 0.82 D with 50 of the 52 control eyes exhibiting refractive errors between +0.69 and + 3.44 D. In contrast, at the end of the treatment period, the treated animals as a group exhibited a much broader range of refractive errors (range = −4.00 to +8.00 D; Fig. 1b) with 42 of the treated eyes exhibiting refractive errors that were more than 2 standard deviations (SDs) away from the control mean.

The limits demarked by the control mean ± 2 SDs (Fig. 1, dashed lines) were used to categorize the spherical-equivalent refractive errors of the experimental monkeys. Using this conservative criterion, 14 and 28 of the treated eyes were classified as hyperopic and myopic, respectively, with 32 treated eyes showing spherical refractive errors that were within the control limits. As

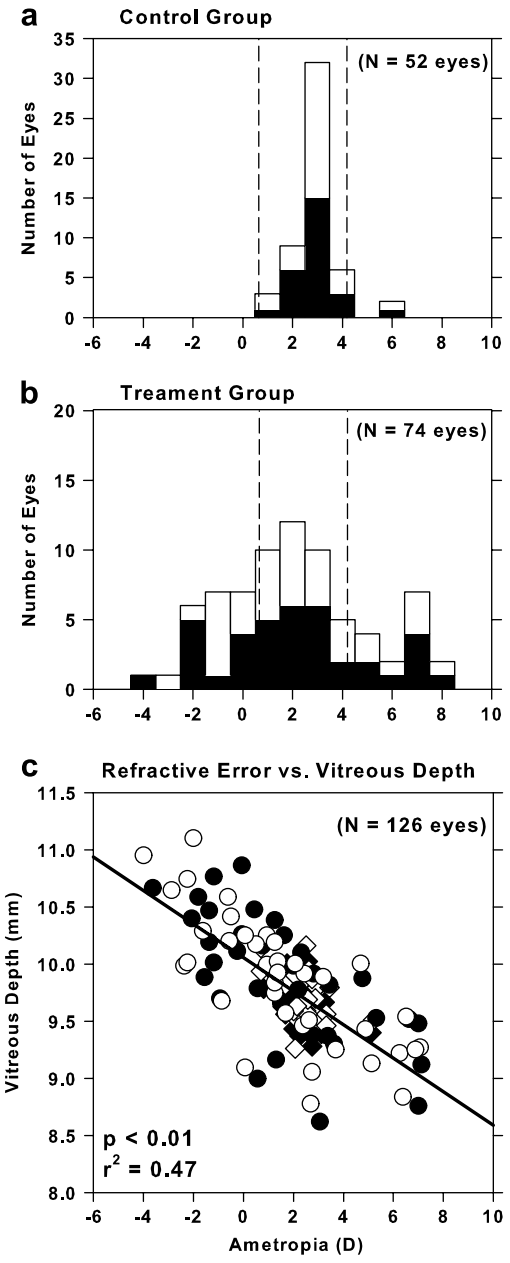

Fig. 1. Refractive error distributions for both eyes (filled bars = right eyes; open bars = left eyes) of (a) 26 normal control animals at ages corresponding to the end of the treatment period (mean = 143 ± 9 days) and (b) 38 treated monkeys at the end of the lens-rearing period (mean = 135 ± 17 days of age). The dashed vertical lines in (a) and (b) represent ±2 standard deviations from the control group mean. (c) Vitreous chamber depth plotted as a function of spherical-equivalent refractive error for all normal (diamonds) and treated eyes (circles). The open and filled symbols represent left and right eyes, respectively. The solid line indicates the best fitting line determined by regression analysis for all the groups taken together.

illustrated in Fig. 1c, the variation in spherical-equivalent refractive errors between subjects was correlated with the eye's axial dimensions, most significantly with vitreous chamber depth (Pearson's correlation coefficient, $r^2 = 0.47$, $P < .01$).

3.2. Effects of abnormal visual experience on high-order aberrations

In addition to having larger refractive errors at the end of the lens-rearing period, the treated monkeys showed larger ranges of coefficient values for each 3rd to 5th order Zernike term and consistently larger overall amounts of high-order aberrations. Fig. 2 illustrates the total amount of high-order aberrations and the amounts of selected high-order aberrations for the right and left eyes of the control and treated animals. With the exception of 3 eyes, where only 1 aberration measure was available, each horizontal tick represents the average aberrations obtained during the two measurement sessions closest to the end of the lens-rearing period. Panel A compares the total RMS errors for the control and treated monkeys. The treated eyes exhibited a larger range of total RMS errors (right eyes, range = 0.17–0.68 μm vs. 0.16–0.26 μm) with 35 of the 74 treated eyes (47%) showing total RMS errors that exceeded the largest RMS error observed in the control monkeys. The mean total RMS error for the treated monkeys was significantly higher than the control mean (right eyes, mean = 0.31 ± 010 μm vs. 0.22 ± 0.03 μm, one-tailed, two-sample t-test, $P = .0001$).

In normal monkeys, spherical aberration and the 3rd order terms, coma and trefoil, are the dominant high-order aberrations (i.e., contribute the most to the eye's total RMS error; see Ramamirtham et al., 2006) and each of these dominant aberrations was influenced by our lens-rearing procedures. Panels 2B–D compare the amounts of coma, trefoil and spherical aberration between the treated and control monkeys. The absolute amount of coma is expressed as the combined RMS errors for terms Z_3^{-1} and Z_3^1; the absolute amount of trefoil is represented by the combined RMS errors for terms Z_3^{-3} and Z_3^3; and spherical aberration is represented by the magnitude of the signed Z_4^0 term. For both coma and trefoil, a substantial proportion of the treated eye values fell outside the range for the control animals and the mean coma and trefoil terms for the treated eyes were significantly larger than those for the control animals (right eyes; mean RMS coma = 0.13 ± 0.05 μm vs. 0.09 ± 0.03 μm; one-tailed, two-sample, t-test, $P = .005$; mean RMS trefoil = 0.15 ± 0.07 vs. 0.10 ± 0.03 μm, $P = .002$). The average amount of spherical aberration (Z_4^0 term) for the treated monkeys differed significantly from zero for both eyes (spherical aberration was the only individual signed Zernike component that was significantly different from zero in treated animals; two- sample t-test, $P = .02$) and the average spherical aberration was significantly more positive in treated eyes than in control eyes (right eyes, treated group = +0.03 ± 0.07 μm, control group = −0.02 ± 0.06 μm, two-sample t-test, $P = .03$). Whereas only 4 of the 16 control eyes (25%) exhibited positive spherical aberration, 54 of the 74 treated eyes (73%) showed positive spherical aberration.

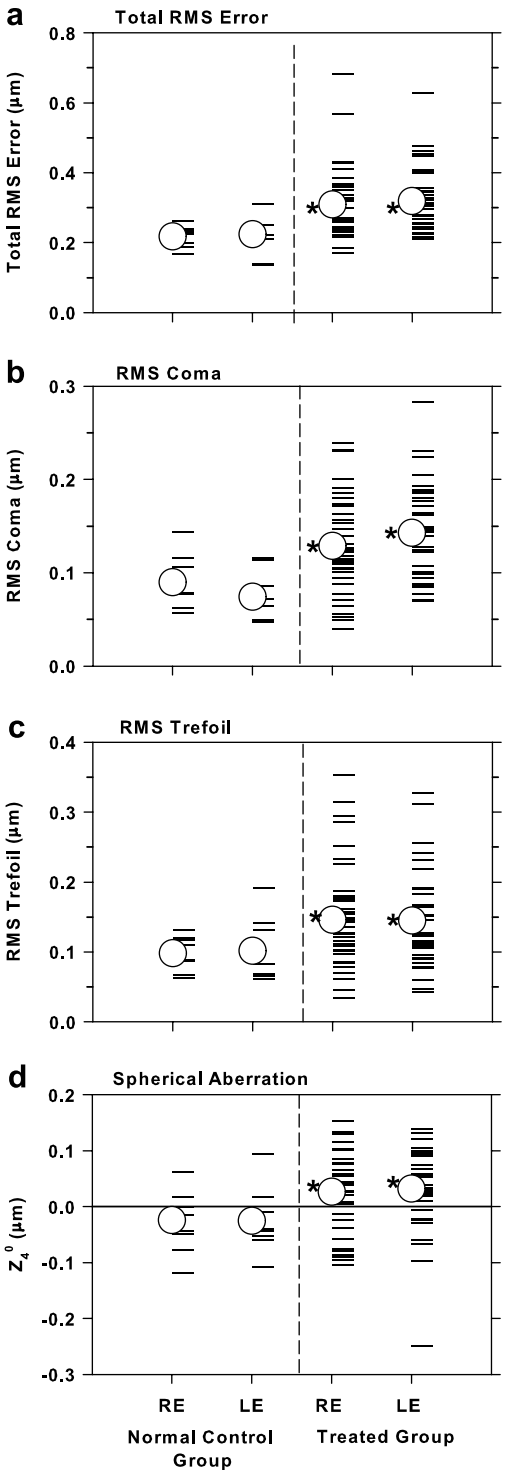

Fig. 2. Total RMS error (a), RMS coma (b), RMS trefoil (c), and the signed values for term Z_4^0 (spherical aberration) (d) for the right and left eyes of individual normal and treated animals. The open circles represent the group means and the asterisks denote treated-group means that were significantly greater than the corresponding control-group mean (one-tailed, two-sample, t-test, $P < .05$).

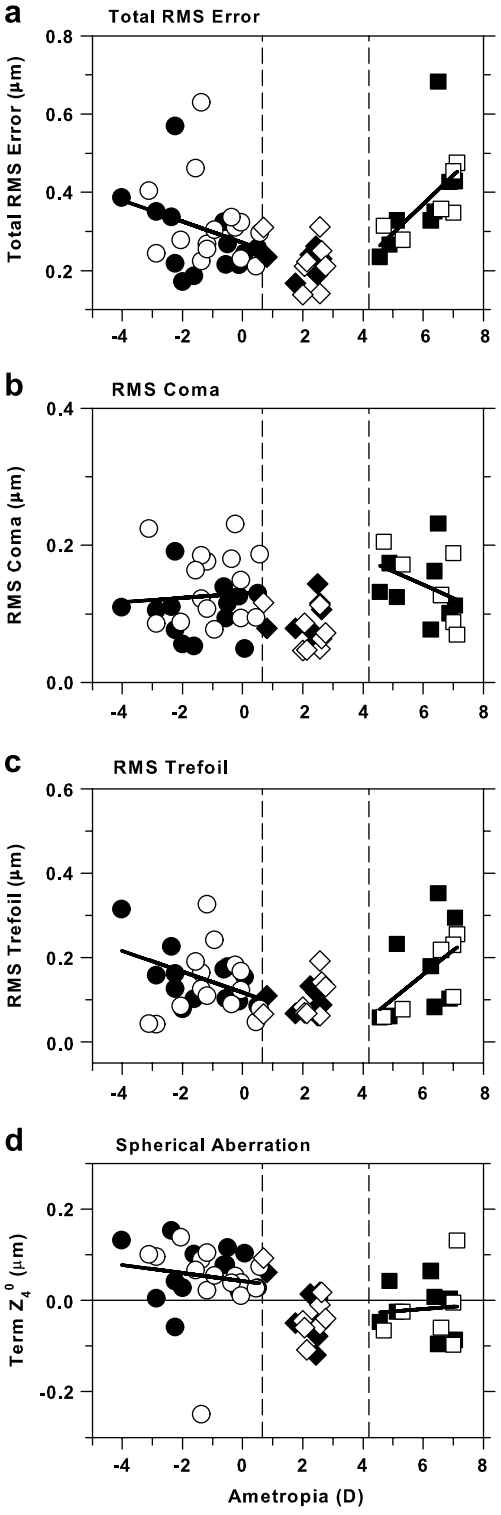

Fig. 3. Total RMS error (a), RMS coma (b), RMS trefoil (c) and spherical aberration (Zernike term Z_4^0) (d) plotted as a function of the spherical-equivalent refractive error for myopic (circles), control (diamonds) and hyperopic groups (squares). The open and filled symbols represent data from right and left eyes, respectively. The solid lines represent linear fits for each group. The vertical dashed lines in each plot denote ±2 standard deviations from the control group mean obtained at ages corresponding to the end of lens-rearing period.

Fig. 3 illustrates the relationship between the magnitude of wavefront aberrations and the degree of spherical-equivalent refractive error, in essence the "axial" ametropia. Specifically, Fig. 3 shows the total RMS error and the absolute amounts of coma (combined RMS errors for the

terms Z_3^{-1} and Z_3^1) and trefoil (combined RMS errors for terms Z_3^{-3} and Z_3^3) and the signed amounts of spherical aberration plotted as a function of the spherical-equivalent ametropia for individual eyes. The plots include data for the right and left eyes of all of the control animals and for the treated eyes that had refractive errors that fell outside the limits defined by the control mean ± 2 SDs. Although all of the monkeys in the hyperopic group wore powered spectacle lens, the monkeys in the myopic group underwent either form deprivation or minus lens treatment. To increase the sample size of myopic monkeys, we have pooled data from myopic animals that were subjected to different rearing regimens. We believe that this strategy was reasonable because, for example, within our myopic group, which included monkeys that experienced form deprivation ($n = 12$ eyes) or hyperopic defocus ($n = 16$ eyes), there were no differences between lens- and diffuser-reared monkeys in the magnitude of myopia, vitreous chamber depth, total RMS error, RMS coma, RMS trefoil or spherical aberration (two-sample t-test, P values = .06–.84). We did not include treated eyes that had spherical-equivalent refractive errors that fell within 2 SDs of the control mean because almost all of these animals had significant amounts of astigmatism, which, as described below, were also associated with larger than normal amounts of wavefront aberrations.

As shown in Fig. 3a, both hyperopic and myopic treated eyes showed a larger range of total RMS wavefront errors than control eyes. The mean total RMS error for the hyperopic treated eyes was significantly higher than that for controls (mean, hyperopes = 0.38 ± 0.11 μm vs. 0.22 ± 0.05 μm, one-way ANOVA, $P = .0001$; Tukey's pairwise comparison, $P < .05$) and there was a significant positive correlation between the amount of wavefront aberrations and the degree of hyperopia (Pearson's correlation coefficient $r = 0.63$, $P = .016$). The mean total RMS errors for the myopic treated eyes was also significantly higher than that for control eyes (myopes = 0.30 ± 0.10 μm vs. 0.22 ± 0.05 μm; Tukey's pairwise comparison, $P < .05$) and although the degree of wavefront aberrations increased with the degree of myopia, this trend was not statistically significant (Pearson's correlation coefficient $r = -0.30$, $P = .12$).

With respect to the dominant high-order Zernike terms, both myopic and hyperopic treated eyes exhibited larger ranges of RMS coma, RMS trefoil, and spherical aberration than control eyes and higher average amounts of these wavefront aberrations (coma: myopes = 0.13 ± 0.05 μm, control = 0.08 ± 0.03 μm, hyperopes = 0.14 ± 0.05 μm; trefoil: myopes = 0.15 ± 0.06 μm, control = 0.10 ± 0.04 μm, hyperopes = 0.17 ± 0.10 μm; spherical aberration: myopes = 0.05 ± 0.07 μm, controls = −0.03 ± 0.06 μm, hyperopes = −0.02 ± 0.07 μm; one-way ANOVA, $P = .001$–.02; Tukey's pairwise comparisons, $P < .05$ for all comparisons with the exception of the mean spherical aberration of hyperopes). Although there was no obvious relationship between the amount of coma and the degree of ametropia for either hyperopic or myopic eyes (Pearson's correlation coefficient, for hyperopes $r = -0.38$, $P = .18$, for myopes $r = 0.08$, $P = .72$), RMS trefoil increased significantly with the degree of myopia and hyperopia (Pearson's correlation coefficient $r = -0.48$, $P = .01$ for myopes, $r = 0.56$, $P = .03$ for hyperopes). Spherical aberration was not significantly correlated with the degree of myopia or hyperopia (Pearson's correlation coefficient $r = -0.14$, $P = .47$ for myopes, $r = 0.08$, $P = .80$ for hyperopes), however, as illustrated in Fig. 3d, there were obvious differences in the sign of spherical aberration between control animals and the myopic treated eyes. With 2 exceptions, the great majority of the myopic eyes (93%) showed positive spherical aberration. In contrast, the majority of control eyes had negative spherical aberration; only 4 of the 16 control eyes showed positive spherical aberration.

The Strehl ratio, which is defined as the ratio of the central intensities of the aberrated point spread function (PSF) and the diffraction-limited PSF, provides an estimate of image quality. Since the treated monkeys could intermittently compensate for spherical defocus through accommodation or near viewing, the Strehl ratio was computed by excluding only the defocus term. In other words, the Strehl ratio was computed using the 2nd order astigmatism terms and the 3rd to 10th high-order terms. Fig. 4 shows box plots of the Strehl ratios for the right and left eyes of the control and treated animals. The average Strehl ratios for the treated eyes were consistently lower than those for control eyes (right eyes, 0.01 ± 0.02 vs. 0.04 ± 0.01, one-tailed, two-sample t-test, $P = .0001$) with both the myopic and hyperopic subgroups showing lower mean ratios (right eyes, myopes = 0.02 ± 0.02; hyperopes = 0.01 ± 0.01, one-way ANOVA, $P = .001$; Tukey's pairwise compari-

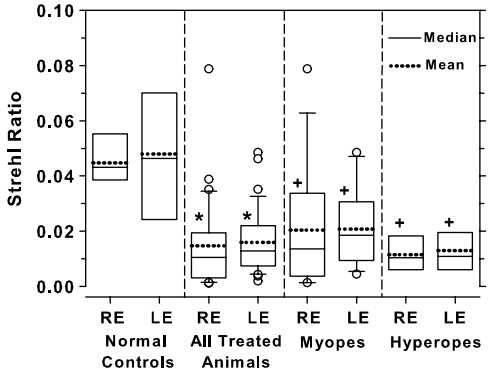

Fig. 4. Box plots of the Strehl ratios for the left and right eyes of the control animals, all of treated animals combined, and the myopic and hyperopic subgroups. The solid and dashed horizontal line inside each box denotes median and mean values, respectively. The edges of the box represent the 25th and 75th percentiles and the extended bars mark the 10th and 90th percentiles. The open circles denote data points that fall outside the 10th to 90th percentile limits. The asterisks (two-sample t-test) and plus symbols (one-way ANOVA and Tukey's pairwise comparisons) indicate that the mean values for a given group were significantly lower than that for the control eyes.

sons, all $P < .05$). Thus, after correcting for defocus, astigmatism and the high-order aberrations resulted in poorer retinal image quality in treated eyes than in control eyes.

At the end of the lens-rearing period, 16 of the 38 treated monkeys (32 eyes) had spherical-equivalent refractive errors that were within 2 SDs of the mean refractive error for the age-equivalent control monkeys (Fig. 1b). Although these animals did not show obvious axial ametropias at the end of the treatment period, several observations indicated that our rearing strategies had altered refractive development. For example, several of these treated animals exhibited anisometropias that were outside the normal range. In other cases, there were obvious deviations from the normal course of emmetropization early in the treatment period, but by the end of the rearing period, the spherical-equivalent refractive errors for these monkeys had returned to within normal limits. However, the most obvious departure from normal was the development of astigmatic refractive errors. As we have previously reported, both form deprivation and optically imposed defocus, produced significant amounts of astigmatism in many of our treated monkeys and this astigmatism reflected changes in the shape of the anterior corneal surface (Kee, Hung, Qiao-Grider, Ramamirtham, & Smith, 2005). Fig. 5a compares the degree of astigmatism at the end of the treatment period for control eyes and the treated eyes that maintained spherical-equivalent refractive errors within the control limits (i.e., "Non-Spherical Ametropic Eyes"). Significant amounts of astigmatism were rare in control eyes. At ages corresponding to the end of the lens-rearing period for the treated monkeys, the mean amount of astigmatism for the control group was 0.13 ± 0.15 D and no control animals exhibited more than 0.37 D of astigmatism. In comparison, 29 of the 32 eyes in the non-spherical ametropic group had astigmatic errors that were outside the control range and the mean astigmatic errors were dramatically higher than those for the control eyes (right eyes, mean $= 1.71 \pm 0.93$ D and left eyes, mean $= 1.14 \pm 0.65$ D, one-way ANOVA, right eyes, $P = .001$, left eyes, $P = .003$; Tukey's pairwise comparisons, all $P < .05$). Similarly, the treated monkeys in the hyperopic and myopic subgroups also exhibited astigmatic errors that were significantly higher than the amounts of astigmatism in control eyes (right eyes, myopes $= 1.11 \pm 0.92$ D, hyperopes $= 0.85 \pm 0.70$ D, Tukey's pairwise comparisons, all $P < .05$). Although there were some differences in the prevalence of astigmatism (refractive astigmatism $\geqslant 1$ D; myopes $= 35\%$; hyperopes $= 29\%$ and non-spherical ametropes $= 62\%$), there were no systematic differences in the range and the average degree of astigmatism between the three treated monkey subgroups (Tukey's pairwise comparison, $P > .05$).

As illustrated in Fig. 5b, the treated monkeys in the non-spherical ametropic group, also exhibited higher total RMS errors than control animals. The right eye mean for the controls was 0.22 ± 0.03 μm whereas for the non-spherical ametropic group, the right eye mean was 0.30 ± 0.07 μm (one-way ANOVA, $P = .02$; Tukey's pairwise comparisons, $P < .05$). Thus, vision-induced alterations in ocular growth, which are also manifest as changes in the shape of the cornea, can contribute to higher than normal aberration levels, even in the absence of an axial ametropia. However, the amount of astigmatism at the end of the treatment period was not significantly correlated with the amount of high-order aberrations in any of the three experimental subgroups or in the population of treated monkeys as a whole (Pearson's correlation coefficient $r = -0.23$ to $+0.35$).

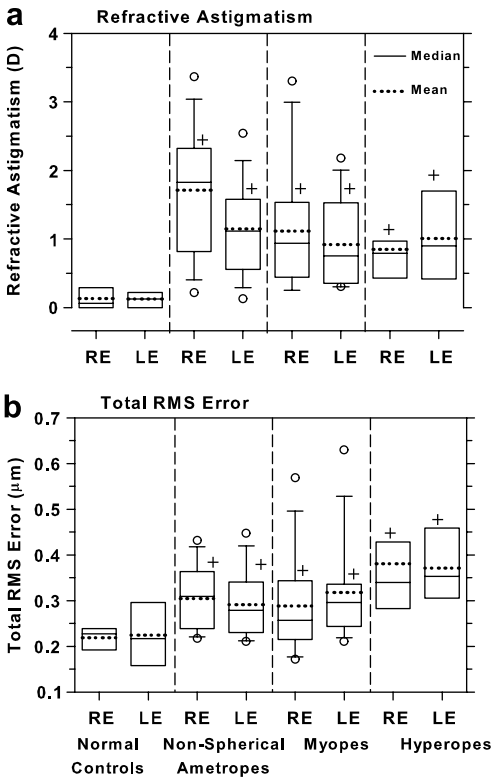

Fig. 5. Box plots of refractive astigmatism (a) and total RMS errors (b) for the right and left eyes of the normal controls, the non-spherical ametropes, the myopes and the hyperopes. The solid and dashed horizontal line inside each box denotes median and mean values, respectively. The edges of the box represent the 25th and 75th percentiles and the extended bars mark the 10th and 90th percentiles. The open circles denote data points that fall outside the 10th to 90th percentile limits. The plus symbols denote group means that were significantly higher than those obtained for the normal controls (one-way ANOVA and Tukey's pairwise comparisons).

3.3. High-order aberrations during the recovery from experimentally induced ametropias

The longitudinal changes in spherical-equivalent refractive error, the degree of astigmatism, and the total RMS wavefront error are illustrated in Fig. 6 for four monkeys that were representative of the group of treated monkeys that we followed until at least 300 days of age. Monkeys MIT and ZAK were selected because both of these monkeys developed abnormal spherical-equivalent refractive

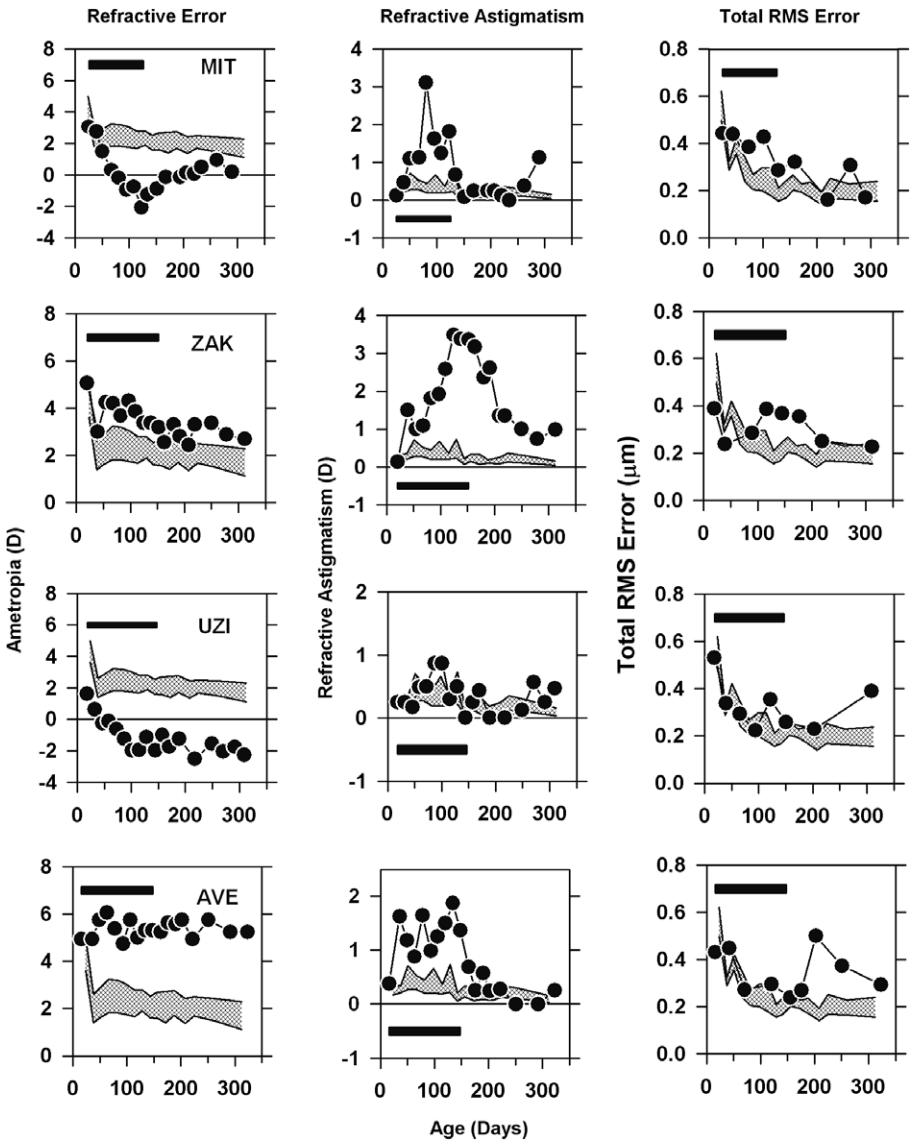

Fig. 6. Spherical-equivalent refractive error (left), refractive astigmatism (middle) and total RMS error (right) plotted as a function of age for 4 representative treated animals that developed axial and astigmatic ametropias. The patterned area represents the 95% confidence intervals for the normal control eyes. The filled horizontal bars demark the lens-rearing period.

errors during the treatment period, but when unrestricted vision was restored (the filled horizontal bars indicate the lens-rearing period), their spherical-equivalent refractive errors decreased to near normal values, i.e., like many young monkeys reared with altered visual experience, these monkeys recovered from the experimentally induced refractive errors and the recovery was complete by about 300 days of age. Monkeys UZI and AVE also developed obvious spherical ametropias during the lens-rearing period, but following the restoration of unrestricted vision there was no evidence of recovery from their spherical-equivalent refractive errors. All four of these monkeys also showed representative astigmatic errors. In particular, all four of these monkeys also developed astigmatic errors during the rearing period that were well outside the control range and in each case the degree of astigmatism decreased to normal values following the rearing period. In some cases, the recovery from these astigmatic errors appeared to be synchronized with the onset of unrestricted vision (e.g., Monkey ZAK and AVE), but as we have previously reported, for some animals (e.g., Monkeys MIT and UZI) the decrease in astigmatism began during the lens-rearing period.

As shown in the right column of Fig. 6, at the start of the lens-rearing period, all 4 of these treated animals showed total RMS wavefront errors that were within the 95% confidence interval for the 5 control animals that were followed longitudinally (the cross hatched areas). The total RMS error for both the control and treated animals decreased with age, however, the decrease was smaller in the treated animals so that by the end of the lens-rearing period all of the treated monkeys showed total RMS errors

that were outside the 95% confidence interval for control animals. Following the onset of unrestricted vision the magnitude of the wavefront aberrations in Monkeys MIT and ZAK, the two animals that recovered from the induced refractive errors, decreased to within the 95% confidence interval for control animals. On the other hand, in the treated monkeys that did not show obvious reductions in their spherical refractive errors following the onset of unrestricted vision, there was a tendency for the magnitude of the wavefront aberrations to increase over time.

Longitudinal data on refractive error and wavefront aberration for approximately the first year of life were obtained from a total of 13 treated monkeys that developed significant spherical ametropias during the lens-rearing period (i.e., ametropias that were more than 2 SDs from the control mean). Fig. 7 summarizes the changes in total RMS error that took place during and after the lens-rearing period for these 13 treated monkeys and for the 5 control monkeys that were followed for at least a year. In Fig. 7, these 13 treated monkeys were separated into 2 subgroups based on whether they recovered from the experimentally induced spherical ametropias. Five of the 13 monkeys showed no signs of recovery. The refractive errors for these 5 monkeys were well outside the age-matched normal range throughout the post-treatment recovery period (“no-recovery” group). On the other hand, 8 of the 13 animals exhibited substantial amounts of recovery from the induced refractive error so that by the end of the observation period, their spherical-equivalent refractive errors were within the age-matched normal range, that is, within 2 SDs of the control mean. The animals that showed no recovery, exhibited on average only 0.45 ± 0.30 D changes in their refractive status during the recovery period (refractive status at the end of the observation period minus refractive status at the end of treatment). While the animals in the recovery group showed on average 1.78 ± 0.95 D (range = 0.81–3.9 D) changes in their spherical-equivalent refractive errors. As illustrated in Fig. 7, prior to the onset of the lens-rearing procedures (mean age $= 23 \pm 10$ days), there were no differences in the average total RMS wavefront errors between the control (circles) and either the recovery (triangles) or no-recovery monkeys (squares) (one-way ANOVA, $P = .47$, Kruskal–Wallis test, $P = .45$). Subsequently, all 3 groups showed a decrease in total RMS errors as a function of age, but, the average decrease for the treated groups was significantly less than that for the control monkeys. Consequently, at the end of the lens-rearing period (mean age $= 140 \pm 17$ days), the magnitude of high-order aberrations in both treated groups was comparable (one-way ANOVA, $P = .026$; Tukey’s pairwise comparison, $P > .05$) and significantly higher than that for the control animals (Tukey’s pairwise comparison, $P < .05$). Following unrestricted vision, the total RMS errors in the recovery group decreased so that by the end of the observation period, the degree of wavefront aberrations in the recovery animals was on average not different from that in the age-matched control animals (one-way ANOVA, $P = .002$; Tukey’s pairwise comparison, $P > .05$). However, the animals that did not recover from the abnormal refractive errors developed higher levels of aberrations during the recovery period and at the end of the observation period, their average total RMS errors were significantly higher than that for the age-matched controls (Tukey’s pairwise comparison, $P < .05$). Thus, recovery of refractive error to normal levels is associated with the recovery of aberrations to normal levels. However, if abnormal refractive errors persist following the restoration of unrestricted clear vision, aberration levels (total RMS error) also remain high.

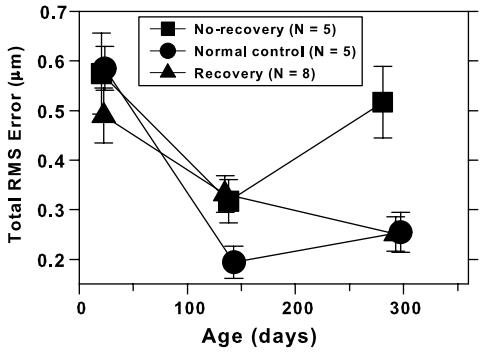

Fig. 7. Mean (±1 SE) total RMS errors plotted as a function of age for control monkeys (circles), treated monkeys that recovered from the experimentally induced refractive errors (triangles), and treated monkeys that did not show recovery from the experimentally induced axial errors. For the treated monkeys, the first and second data points represent values obtained at the start and end of the lens-rearing period.

4. Discussion

Our results show that shortly after birth, both normal monkeys and infant monkeys that were subjected to abnormal visual experience showed a decrease in the magnitude of high-order aberrations with age. However, the decrease in aberrations was typically smaller in the treated animals. Consequently, at the end of the lens-rearing period, higher than normal amounts of aberrations were observed in treated eyes, both hyperopic and myopic eyes and treated eyes that developed astigmatism, but not spherical ametropias. The total RMS wavefront error increased with the degree of spherical refractive error, but was not correlated with the degree of astigmatism. Both myopic and hyperopic treated eyes showed elevated amounts of coma and trefoil and the degree of trefoil increased with the degree of spherical ametropia. Myopic eyes also exhibited a much higher prevalence of positive spherical aberration than normal or treated hyperopic eyes. The high amounts of aberrations in the treated eyes were, however, not necessarily permanent. Following the onset of unrestricted vision, the amount of high-order aberrations decreased in the experimental monkeys that also recovered from the experimentally induced refractive errors.

4.1. Comparisons with previous studies in animals and humans

There are similarities between our results and those from other animal studies. For example, chicks that developed myopia as a result of form deprivation (Garcia de la Cera et al., 2006) or hyperopic defocus (Kisilak et al., 2006) also exhibited higher than normal total RMS errors and the treated myopic eyes of monocularly form-deprived marmosets showed higher amounts of wavefront aberrations relative to their fellow non-treated eyes (Coletta et al., 2004). In addition, rearing chicks under constant light conditions, a rearing strategy that produces hyperopia and obvious anterior segment changes, results in elevated high-order aberrations (Howland et al., 2004). There were also similarities in the pattern of changes in high-order aberrations. Like our treated monkeys, myopic chicks exhibited significant increases in both 3rd and 4th order aberrations. However, there were some differences in the nature of the aberration changes between our monkeys and chicks. For example whereas our myopic monkeys developed positive spherical aberration, Garcia de la Cera et al. (2006) found that chicks with form deprivation myopia developed negative spherical aberration. It seems likely that these kinds of disparities reflect interspecies differences in ocular anatomy and the specific manner in which visual experience influences eye growth and shape. Regardless, the main point is that alterations in visual experience that are sufficient to alter an eye's refractive error also promote the development of larger amounts of monochromatic wavefront aberrations in macaque monkeys, marmosets, and chicks.

Although some human studies have failed to find an association between refractive errors, in particular myopia, and either the pattern or amount of high-order aberrations (Carkeet et al., 2002; Cheng et al., 2003; Legras et al., 2004; Porter et al., 2001), the results of other studies are qualitatively and quantitatively similar to our findings in macaque monkeys with induced refractive errors. For example, in comparison to emmetropes, higher total RMS errors have been found in adult humans with myopia (Collins et al., 1995; He et al., 2002; Llorente et al., 2004; Paquin et al., 2002), hyperopia (Llorente et al., 2004), and astigmatism (Cheng et al., 2003). Moreover, in comparison to emmetropes, it has been reported that human myopes have higher amounts of coma and positive spherical aberration. And despite the obvious methodological differences between our study and those involving human subjects, the absolute and relative magnitudes of aberrations in ametropic monkey and human eyes were comparable. For example, in our myopic monkeys the range of total RMS errors varied from 0.17 to 0.62 μm with an average of 0.30 μm, which was 0.08 μm larger than that found in control monkeys. In myopic humans, Llorente et al. (2004) reported that the average total RMS error was 0.32 μm (pupil diameter = 6.5 mm); Paquin et al. (2002) found a range of 0.2–0.53 μm (pupil diameter = 5.0 mm); and He et al. (2002) found that the average difference between myopic and emmetropic humans was 0.07 μm (pupil diameter = 6.0 mm). Thus, monkeys with experimentally induced refractive errors exhibit alterations in high-order aberrations that are very comparable to those observed in humans with natural ametropias.

Assuming that the mechanisms responsible for aberrations in ametropic monkeys and humans are similar, our results provide several potential explanations for the inconsistencies observed in human studies. In monkeys, the amount of aberrations varied with the magnitude of spherical refractive error; astigmatic eyes without spherical-equivalent refractive errors had substantial amounts of aberrations; and even with controlled rearing regimens, there was substantial intersubject variability. These results suggest that large, diverse samples are needed to distinguish potential differences in high-order aberrations between eyes with spherical ametropias and emmetropic eyes and that the potential confounding effects of astigmatism should be considered when comparing aberrations between myopes or hyperopes and emmetropes. Thus, differences in subject populations could have contributed to the inconsistencies found in human studies. It is also potentially important that the high-order aberrations that developed in association with vision-induced refractive errors in monkeys were not always permanent. In particular, following the onset of unrestricted vision, the aberrations decreased in concert with the recovery from experimentally induced refractive errors in some animals. In this respect, the weight of evidence suggests that the higher amounts of aberrations reflect structural changes associated with the development of refractive error and that the aberrations should persist as long as the refractive error was stable. However, it is possible that the amounts of high-order aberrations in humans are larger during the time period when anomalous refractive errors are progressing or emerging. Thus, a subject's age and refractive error history (possibly the relative stability of refractive errors) may also influence the relationship between refractive errors and aberrations.

4.2. Structural correlates of high-order aberrations in treated monkeys

In normal monkeys, high-order aberrations decrease in a monotonic fashion during the first 150 days of life. Although some of the reduction in aberrations during emmetropization may reflect a geometric increase in the overall scale of the eye, model predictions indicate that scale changes alone cannot account for all of the changes in high-order aberrations (Ramamirtham et al., 2006) and longitudinal measures of ocular parameters in monkeys and humans show that the adult/adolescent eye is not simply a scaled version of the infant eye, i.e., eye growth is not uniform (Qiao-Grider et al., 2007). Consequently, some of the decrease in high-order aberrations in normal monkeys must be due to changes in the shape and organization of the eye's optical components (Rama-

mirtham et al., 2006). Geometric scaling can also not explain the increase in high-order aberrations found in ametropic monkeys. If the alterations in aberrations in our experimental monkeys were due simply to uniform changes in eye size, then the degree of high-order aberrations should have been directly correlated with axial length, i.e., myopes should exhibit higher aberrations than emmetropes and hyperopes. However, we found that both longer myopic and shorter hyperopic eyes exhibited higher than normal levels of high-order aberrations. Thus, a simple geometrical difference in eye length cannot explain higher than normal levels of aberrations in myopic and hyperopic eyes. It is also obvious that the association between astigmatism and high-order aberrations in our experimental monkeys cannot be accounted for by uniform scaling changes.

When comparing high-order aberrations between subjects, it is important that the individual wavefront maps are centered on the same reference axis, specifically the line of sight. We identified the presumed line of sight in our anesthetized monkeys based on the Hirschberg estimates made by Quick and Boothe (1989, 1992) and assumed that angle lambda was the same in all monkeys. However, in humans, it has been reported that angle lambda varies with age (London & Wick, 1982) and with the eye's refractive state and axial length; specifically that in comparison to emmetropes, myopes and hyperopes exhibit smaller and larger angles lambda, respectively (Bansal, Coletta, Moskowitz, & Han, 2004; LeGrand & ElHage, 1980). Consequently, if similar relationships exist in monkeys, it is possible that our data are influenced by these trends. However, the auto-compensation mechanism described by Artal et al. (2006) would tend to mask any alignment errors, at least for lateral coma. Moreover, direct estimates of alignment errors indicate that the potential confounding effects would be small. For example, we compared aberrations measurements in adolescent monkeys made along the pupillary axis with those made along the presumed line of sight, i.e., the measurement axis was displaced 0.3 mm between the two measures. There were no significant differences between the pupillary axis and the presumed line of sight measurements in terms of the total RMS error, RMS coma, RMS trefoil, spherical aberration or any of the individual 3rd to 5th order Zernike terms (two-sample t-test, range of P values = .25–.92). The absolute difference in total RMS error between the pupillary axis and the presumed line of sight was only 0.01 μm, which is small compared to the differences in total RMS errors observed between ametropic and normal control subjects. Assuming that refractive error affects angle lambda similarly in monkeys and humans (Bansal et al., 2004), the largest alignment error that would occur in our population of ametropic monkeys, expressed in terms of the position of the corneal reflex, would be approximately 0.15 mm (based on a 6 D difference in refractive error). Likewise, assuming that the magnitude of the age-dependent changes in angle lambda are similar in monkeys and humans, the maximum alignment error associated with age differences would be about 0.17 mm. Alignment errors of these magnitudes would be negligible and would not substantially alter our conclusions.

The elevated levels of high-order aberrations in the ametropic eyes of our experimental monkeys probably reflect changes in the shapes and relative positions of the eye's optical components. It is well established that vision-induced spherical refractive errors occur primarily as a result of alterations in axial elongation rates, particularly vitreous chamber elongation rates. However, the expansion of the posterior segment of the globe is not necessarily symmetrical. In comparison to emmetropic eyes, adult myopic eyes exhibit greater dimensional increases in the vertical meridian than in the horizontal meridian (Atchison et al., 2005) and naso-temporal asymmetries along the horizontal meridian have been observed in the more myopic eyes of Caucasians with anisomyopia (Logan, Gilmartin, Wildsoet, & Dunne, 2004). The changes in peripheral refractive error that occur in normal infant monkeys during emmetropization also suggest that there are naso-temporal asymmetries in the expansion of the posterior globe of monkeys during normal development (Hung, Ramamirtham, Huang, Qiao-Grider, & Smith, 2006). Thus, it might be expected that either increasing or decreasing axial elongation rates would alter the overall shape of the eye in comparison to a normal emmetropic eye. The potential meridional variations in diameter that result might affect the shape of the crystalline lens or its position or alignment with respect to the cornea. In this respect, alterations in the alignment of the optical centers of the cornea and lens, changes in the position of the pupil, or changes in the projection of the visual axis produced by relative changes in the position of the fovea could alter the amount and pattern of 3rd order aberrations (especially coma-like terms). Alterations in the tilt of the crystalline lens, by changing the relative alignment of the anterior and posterior lens sutures, could change the pattern of trefoil (Kuszak, Zoltoski, & Tiedemann, 2004; Thibos et al., 2002b). It is also clear that alterations in visual experience that are sufficient to produce refractive errors in infant monkeys also influence the anterior segment of the eye. In particular, almost all of our experimental monkeys exhibited higher than normal amounts of astigmatism, which demonstrates that our rearing regimens produced asymmetrical changes in corneal shape and the anatomy of the anterior segment. The failure to find a significant correlation between the total RMS error and the degree of astigmatism may reflect confounding effects of aberrations associated with lenticular changes.

There are several possible explanations for differences in the sign and amount of spherical aberration observed between myopic monkeys and non-myopic monkeys. If myopic and emmetropic eyes had identical optical components and differed only in axial length then, as Cheng et al. (2003) have argued, SHWS instruments would falsely measure more positive spherical aberration in myopic eyes than in emmetropic eyes. However, we have previously shown

that altered visual experience can produce changes in the anterior segment, specifically in the anterior cornea (Kee et al., 2005). Thus, it is possible that the differences in spherical aberration, particularly the sign of spherical aberration, between myopes and non-myopes reflect vision-induced differences in the surface curvature profiles of the cornea and/or crystalline lens. The more positive spherical aberration profiles found in myopic monkeys could reflect changes in peripheral corneal curvature.

The lens could also contribute to the increase in spherical aberration. We have previously shown that there are no significant interocular differences in the central thickness of the crystalline lens, the central anterior and posterior lens curvatures, and equivalent refractive indices of the lens between the eyes in anisometropic monkeys (Qiao-Grider et al., 2002). Thus, many aspects of the crystalline lens do not appear to be significantly altered during the development of refractive errors. However, we cannot rule out the possibility that peripheral lens curvature and/or the refractive index gradient of the lens are altered during the development of abnormal refractive errors. Priolo et al. (2000) observed larger than normal magnitudes of spherical aberration in the isolated crystalline lenses of form deprivation induced myopic chicks and attributed these elevated aberration levels to alterations in the refractive indices of the lens. Comparing the anterior corneal asphericities and computing wavefront aberrations of the individual optical components of the eye for different refractive groups could potentially provide clues to the origin of positive spherical aberration that is observed in myopic monkeys.

If the increase in aberrations in ametropic eyes reflects changes in the shape of the eye, then the decrease in aberrations that was associated with the recovery from abnormal refractive errors suggests that during the recovery process the eye assumes a more normal shape or that at least the eye's optical components do. Recovery from spherical refractive errors in infant monkeys is mediated primarily by alterations in vitreous chamber elongation rate; in terms of spherical-equivalent power, the cornea and presumably the lens appear to follow a normal growth trajectory during recovery. For example, during the recovery from myopia, vitreous chamber elongation is reduced below normal levels and the spherical refractive error decreases because the cornea and lens continue to decrease in power as in normal eyes (Qiao-Grider, Hung, Kee, Ramamirtham, & Smith, 2004). However, the fact that corneal astigmatism also decreases during the recovery process, indicates that the cornea must return to a more normal shape. In this respect, it is likely that any potential misalignment or changes in lens shape also returned to a more normal state during recovery.

4.3. Relationship between high-order aberrations and refractive errors

It has been suggested that the association between greater amounts of high-order aberrations and refractive error comes about because the visual consequences of aberrations induce ametropic growth, in particular that the increase in image degradation associated with higher than normal aberrations would promote axial elongation via the mechanisms responsible for the phenomenon of form deprivation myopia (Charman, 2005; Collins et al., 1995; He et al., 2002; Paquin et al., 2002). In our monkeys, increased aberrations were observed in myopic, hyperopic, and astigmatic monkeys and the patterns of aberrations in our experimental monkeys were similar to those described in humans with natural refractive errors. Given that all types of refractive errors showed increased aberrations argues against the idea that a simple form-deprivation model is responsible for the association between refractive errors and high-order aberrations. Moreover, the fact that experimental animals that exhibited increased high-order aberrations could recover from experimentally induced refractive errors, a process that is mediated by visual feedback associated with the eye's refractive error (Norton, Amedo, & Siegwart, 2006; Troilo & Wallman, 1991; Wildsoet & Schmid, 2000), suggests that the presence of higher levels of high-order aberrations does not prevent the eye from responding to defocus. When one considers the relative magnitude of the high-order aberrations associated with moderate refractive errors, the dominance of optical defocus over high-order aberrations is not surprising. For example, at the end of the treatment period the average differences in total RMS error between control animals and experimental animals with myopia and hyperopia was 0.08 and 0.15 μm, respectively. When expressed in terms of equivalent spherical defocus, these magnitudes of wavefront error represent relative increases in defocus of only 0.10 and 0.17 D, respectively. It would seem that such low magnitudes of blur would be unlikely to significantly alter refractive development, since the eye routinely experiences much larger amounts of blur in real life situations. For example, the average amount of accommodative lag for a 3 D stimulus in emmetropic children and young adults is about 0.40–0.80 D which is much larger than the equivalent blur due to high-order aberrations in ametropic eyes (Gwiazda, Thorn, Bauer, & Held, 1993; Rosenfield & Gilmartin, 1999; Seidemann & Schaeffel, 2003; Wang & Ciuffreda, 2006).

Several observations support the hypothesis that the association between high-order aberrations and refractive error exists because the ocular changes associated with the development of a refractive error lead to an increase in high-order aberrations. First, every experimental eye that showed increased amounts of high-order aberrations also exhibited either significant spherical and/or astigmatic refractive errors. We failed to find any experimental eyes with increased aberrations, but no refractive error. Second, at the end of the treatment period, the amount of high-order aberrations was positively correlated with the degree of axial ametropia. And third, animals that failed to recover from the induced refractive errors following the onset of unrestricted vision also continued to exhibit larger

than normal amounts of high-order aberrations. On the other hand, the aberrations decreased in eyes that recovered from the induced refractive errors.

We found little evidence to support the hypothesis that there are vision-dependent mechanisms that use visual feedback to reduce the total amount of ocular aberrations. All of our treated animals were subjected to substantial changes in visual experience as a result of our experimental rearing regimens (e.g., form deprivation). However, every experimental animal exhibited an absolute decrease in the total amount of aberrations during the treatment period. Although the magnitude of this decrease was, on average, smaller than that in control animals, it occurred despite substantial reductions in retinal image quality caused as a result of imposed defocus or form deprivation. Thus, at least a significant part of the early decrease in high-order aberrations occurs passively and is independent of the nature of visual experience. Moreover, there were numerous examples of treated eyes that experienced substantial amounts of defocus or form deprivation, yet developed a normal aberration profile. Consequently, if these vision-dependent mechanisms exist, they can, at least in some animals, operate normally in the presence of substantial amounts of defocus or form deprivation. However, it seems more likely that the low levels of aberrations in these ametropic animals reflect the action of passive, auto-compensation mechanisms similar to those described by Artal et al. (2006).

In conclusion, our results show that high-order aberrations are influenced by the vision-dependent mechanisms that regulate refractive development. In particular, the increase in high-order aberrations in our monkeys with anomalous refractive errors appears to be an optical byproduct of the vision-induced alterations in ocular growth that underlie the changes in refractive error. Overall, the results from our study suggest that the higher amounts of wave aberrations observed in ametropic humans are a consequence, rather than a cause, of abnormal refractive development.

References

Artal, P., Benito, A., & Tabernero, J. (2006). The human eye is an example of robust optical design. *Journal of Vision, 6*, 1–7 http://journalofvision.org/6/1/1/.

Artal, P., Guirao, A., Berrio, E., & Williams, D. R. (2001). Compensation of corneal aberrations by the internal optics in the human eye. *Journal of Vision, 1*, 1–8.

Atchison, D. A. (2004). Anterior corneal and internal contributions to peripheral aberrations of human eyes. *Journal of Optical Society of America A, Optics, Images, Science, and Vision, 21*, 355–359.

Atchison, D. A., Pritchard, N., Schmid, K. L., Scott, D. H., Jones, C. E., & Pope, J. M. (2005). Shape of the retinal surface in emmetropia and myopia. *Investigative Ophthalmology and Vision Science, 46*, 2698–2707.

Bansal, J., Coletta, N. J., Moskowitz, A., & Han, H. (2004). Pupil displacement in corneal topography images is related to the eye's refractive error. *Investigative Ophthalmology and Vision Science, 45*(Suppl.) [ARVO E-Abstract nr. 2762].

Bradley, D. V., Fernandes, A., Lynn, M., Tigges, M., & Boothe, R. G. (1999). Emmetropization in the rhesus monkey (*Macaca mulatta*). birth to young adulthood. *Investigative Ophthalmology and Vision Science, 40*, 214–229.

Calderone, L., Grimes, P., & Shalev, M. (1986). Acute reversible cataract induced by xylazine and by ketamine-xylazine anesthesia in rats and mice. *Experimental Eye Research, 42*, 331–337.

Campbell, F. W., & Gubisch, R. W. (1966). Optical quality of the human eye. *Journal of Physiology, 186*, 558–578.

Carkeet, A., Luo, H. D., Tong, L., Saw, S. M., & Tan, D. T. (2002). Refractive error and monochromatic aberrations in Singaporean children. *Vision Research, 42*, 1809–1824.

Castejon-Mochon, J. F., Lopez-Gil, N., Benito, A., & Artal, P. (2002). Ocular wave-front aberration statistics in a normal young population. *Vision Research, 42*, 1611–1617.

Charman, W. N. (1991). Wavefront aberration of the eye: A review. *Optometry and Vision Science, 68*, 574–583.

Charman, W. N. (2005). Aberrations and myopia. *Ophthalmic and Physiological Optics, 25*, 285–301.

Cheng, H., Barnett, J. K., Vilupuru, A. S., Marsack, J. D., Kasthurirangan, S., Applegate, R. A., et al. (2004). A population study on changes in wave aberrations with accommodation. *Journal of Vision, 4*, 272–280http://journalofvision.org/4/4/3/.

Cheng, X., Bradley, A., Hong, X., & Thibos, L. N. (2003). Relationship between refractive error and monochromatic aberrations of the eye. *Optometry and Vision Science, 80*, 43–49.

Coletta, N. J., Marcos, S., Wildsoet, C., & Troilo, D. (2003). Double-pass measurement of retinal image quality in the chicken eye. *Optometry and Vision Science, 80*, 50–57.

Coletta, N. J., Triolo, D., Moskowitz, A., Nickla, D. L., & Marcos, S. (2004). Ocular wavefront aberrations in the awake marmoset. *Investigative Ophthalmology and Vision Science, 45*(Suppl.) [ARVO E-Abstract nr. 4298].

Collins, M. J., Wildsoet, C. F., & Atchison, D. A. (1995). Monochromatic aberrations and myopia. *Vision Research, 35*, 1157–1163.

De Brabander, J., Hendricks, T., Chateau, N., Munnik, M., Harms, F., van der Horst, F., et al. (2004). Ametropia and higher order Aberrations in Children 12–13 years of age. *Investigative Ophthalmology and Vision Science, 45*(Suppl.) [ARVO Abstract nr. 2761].

de la Cera, E. G., Rodriguez, G., Llorente, L., Schaeffel, F., & Marcos, S. (2006). Optical aberrations in the mouse eye. *Vision Research, 46*, 2546–2553.

Garcia de la Cera, E., Rodriguez, G., & Marcos, S. (2006). Longitudinal changes of optical aberrations in normal and form-deprived myopic chick eyes. *Vision Research, 46*, 579–589 [Epub 2005 Jul 2026].

Gwiazda, J., Thorn, F., Bauer, J., & Held, R. (1993). Myopic children show insufficient accommodative response to blur. *Investigative Ophthalmology and Vision Science, 34*, 690–694.

Harris, W. F. (1988). Algebra of sphero-cylinders and refractive errors, and their means, variance, and standard deviation. *American Journal of Optometry and Physiological Optics, 65*, 794–802.

He, J. C., Burns, S. A., & Marcos, S. (2000). Monochromatic aberrations in the accommodated human eye. *Vision Research, 40*, 41–48.

He, J. C., Sun, P., Held, R., Thorn, F., Sun, X., & Gwiazda, J. E. (2002). Wavefront aberrations in eyes of emmetropic and moderately myopic school children and young adults. *Vision Research, 42*, 1063–1070.

Howland, B., & Howland, H. C. (1976). Subjective measurement of high-order aberrations of the eye. *Science, 193*, 580–582.

Howland, H. C., & Howland, B. (1977). A subjective method for the measurement of monochromatic aberrations of the eye. *Journal of Optical Society of America, 67*, 1508–1518.

Howland, H. C., Tong, L., Yoko, H., & Toshifumi, M. (2004). High order wave aberration of chicks due to constant light rearing and its recovery. *10th International myopia conference—Abstract*, 1, 21.

Hung, L.-F., Crawford, M. L. J., & Smith, E. L. III, (1995). Spectacle lenses alter eye growth and the refractive status of young monkeys. *Nature Medicine, 1*, 761–765.

Hung, L.-F., Ramamirtham, R., Huang, J., Qiao-Grider, Y., & Smith, E. L. III, (2006). Peripheral refraction in normal infant rhesus monkeys. *Ophthalmic and Physiological Optics, 26*(Suppl.), S052 [Abstract].

Jenkins, T. C. (1963). Aberrations of the Eye and Their Effects On Vision. II. *British Journal of Physiological Optics, 20*, 161–201.

Kee, C. S., Hung, L.-F., Qiao-Grider, Y., Ramamirtham, R., & Smith, E. L. III, (2005). Astigmatism in monkeys with experimentally induced myopia or hyperopia. *Optometry and Vision Science, 82*, 248–260.

Kee, C. S., Hung, L.-F., Qiao-Grider, Y., Ramamirtham, R., Winawer, J., Wallman, J., et al. (2007). Temporal constraints on experimental emmetropization in infant monkeys. *Investigative Ophthalmology and Vision Science, 48*, 957–962.

Kee, C. S., Hung, L.-F., Qiao-Grider, Y., Roorda, A., & Smith, E. L. III, (2004). Effects of Optically Imposed Astigmatism on Emmetropization in Infant Monkeys. *Investigative Ophthalmology and Vision Science, 45*, 1647–1659.

Kelly, J. E., Mihashi, T., & Howland, H. C. (2004). Compensation of corneal horizontal/vertical astigmatism, lateral coma, and spherical aberration by internal optics of the eye. *Journal of Vision, 4*, 262–271http://journalofvision.org/4/4/2/.

Kisilak, M. L., Campbell, M. C., Hunter, J. J., Irving, E. L., & Huang, L. (2006). Aberrations of chick eyes during normal growth and lens induction of myopia. *Journal of Comparitive Physiology. A, Neuroethology, Sensory, Neural, and Behavioral Physiology, 192*, 845–855.

Kroger, R. H. H., Campbell, M. C. W., & Fernald, R. D. (2001). The development of the crystalline lens is sensitive to visual input in the African cichlid fish, *Haplochromis burtoni*. *Vision Research, 41*, 549.

Kuszak, J. R., Zoltoski, R. K., & Tiedemann, C. E. (2004). Development of lens sutures. *International Journal of Developmental Biology, 48*, 889–902.

LeGrand, Y., & ElHage, S. G. (1980). In *Physiological optics. Springer series in optical sciences* (Vol. 13). Berlin: Springer.

Legras, R., Chateau, N., & Charman, W. N. (2004). Assessment of just-noticeable differences for refractive errors and spherical aberration using visual simulation. *Optometry and Vision Science, 81*, 718–728.

Liang, J., Grimm, B., Goelz, S., & Bille, J. F. (1994). Objective measurement of wave aberrations of the human eye with the use of a Hartmann–Shack wave-front sensor. *Journal of Optical Society of America A, Optics, Images, Science, and Vision, 11*, 1949–1957.

Liang, J., & Williams, D. R. (1997). Aberrations and retinal image quality of the normal human eye. *Journal of Optical Society of America A, Optics, Images, Science, and Vision, 14*, 2873–2883.

Llorente, L., Barbero, S., Cano, D., Dorronsoro, C., & Marcos, S. (2004). Myopic versus hyperopic eyes: Axial length, corneal shape and optical aberrations. *Journal of Vision, 4*, 288–298http://journalofvision.org/4/4/5/.

Logan, N. S., Gilmartin, B., Wildsoet, C. F., & Dunne, M. C. (2004). Posterior retinal contour in adult human anisomyopia. *Investigative Ophthalmology and Vision Science, 45*, 2152–2162.

London, R., & Wick, B. C. (1982). Changes in angle lambda during growth: Theory and clinical applications. *American Journal of Optometry and Physiological Optics, 59*, 568–572.

Mahajan, V. (1991). Aberration theory made simple. In O. S. DC (Ed.), *Tutorial texts in optical engineering* (pp. 92–110). Washington, DC: SPIE Optical Engineering Press.

Napper, G. A., Brennan, N. A., Barrington, M., Squires, M. A., Vessey, G. A., & Vingrys, A. J. (1997). The effect of an interrupted daily period of normal visual stimulation on form deprivation myopia in chicks. *Vision Research, 37*, 1557–1564.

Norton, T. T. (1999). Animal models of myopia: Learning how vision controls the size of the eye. *National Research Council, Institute of Laboratory Animal Resources Journal, 40*, 59–77.

Norton, T. T., Amedo, A. O., & Siegwart, J. T. Jr, (2006). Darkness causes myopia in visually experienced tree shrews. *Investigative Ophthalmology and Vision Science, 47*, 4700–4707.

Norton, T. T., & Siegwart, J. T. Jr, (1995). Animal models of emmetropization: Matching axial length to the focal plane. *Journal of American Optometry, 66*, 405–414.

Paquin, M. P., Hamam, H., & Simonet, P. (2002). Objective measurement of optical aberrations in myopic eyes. *Optometry and Vision Science, 79*, 285–291.

Porter, J., Guirao, A., Cox, I. G., & Williams, D. R. (2001). Monochromatic aberrations of the human eye in a large population. *Journal of Optical Society of America A, Optics, Images, Science, and Vision, 18*, 1793–1803.

Priolo, S., Sivak, J. G., Kuszak, J. R., & Irving, E. L. (2000). Effects of experimentally induced ametropia on the morphology and optical quality of the avian crystalline lens. *Investigative Ophthalmology and Vision Science, 41*, 3516–3522.

Qiao-Grider, Y., Hung, L.-F., Kee, C. S., Ramamirtham, R., & Smith, E. L. III, (2007). Normal ocular development in young rhesus monkeys (*Macaca mulatta*). *Vision Research, 47*, 1424–1444.

Qiao-Grider, Y., Hung, L. F., Kee, C. S., Ramamirtham, R., & Smith, E. L. III, (2002). Ocular changes in anisometropic infant rhesus monkeys. *Investigative Ophthalmology and Vision Science, 43*(Suppl.) [ARVO Abstract nr. 2927].

Qiao-Grider, Y., Hung, L. F., Kee, C. S., Ramamirtham, R., & Smith, E. L. III, (2004). Recovery from form deprivation myopia in rhesus monkeys (*Macaca mulatta*). *Investigative Ophthalmology and Vision Science, 45*, 3361–3372.

Quick, M. W., & Boothe, R. G. (1989). Measurement of binocular alignment in normal monkeys and in monkeys with strabismus. *Investigative Ophthalmology and Vision Science, 30*, 1159–1168.

Quick, M. W., & Boothe, R. G. (1992). A photographic technique for measuring horizontal and vertical eye alignment throughout the field of gaze. *Investigative Ophthalmology and Vision Science, 33*, 234–246.

Radhakrishnan, H., Pardhan, S., Calver, R. I., & O'Leary, D. J. (2004). Effect of positive and negative defocus on contrast sensitivity in myopes and non-myopes. *Vision Research, 44*, 1869–1878.

Ramamirtham, R., Kee, C. S., Hung, L.-F., Qiao-Grider, Y., Roorda, A., & Smith, E. L. III, (2006). Monochromatic ocular wave aberrations in young monkeys. *Vision Research, 46*, 3616–3633.

Rosenfield, M., & Gilmartin, B. (1999). Accommodative error, adaptation and myopia. *Ophthalmic and Physiological Optics, 19*, 159–164.

Salmon, T. O., & Thibos, L. N. (2002). Videokeratoscope-line-of-sight misalignment and its effect on measurements of corneal and internal ocular aberrations. *Journal of Optical Society of America A, Optics, Images, Science, and Vision, 19*, 657–669.

Schmid, K. L., & Wildsoet, C. F. (1996). Effects on the compensatory responses to positive and negative lenses of intermittent lens wear and ciliary nerve section in chicks. *Vision Research, 36*, 1023–1036.

Seidemann, A., & Schaeffel, F. (2003). An evaluation of the lag of accommodation using photorefraction. *Vision Research, 43*, 419–430.

Smirnov, M. S. (1961). Measurement of the wave aberration of the human eye. *Biofizika, 6*, 776–795.

Smith, E. L. III, (1998a). Environmentally induced refractive errors in animals. In M. Rosenfield & B. Gilmartin (Eds.), *Myopia and nearwork* (pp. 57–90). Oxford: Butterworth-Heinemann.

Smith, E. L. III, (1998b). Spectacle lenses and emmetropization: The role of optical defocus in regulating ocular development. *Optometry and Vision Science, 75*, 388–398.

Smith, E. L., III, & Hung, L.-F. (1999). The role of optical defocus in regulating refractive development in infant monkeys. *Vision Research, 39*, 1415–1435.

Smith, E. L., III, Kee, C. S., Ramamirtham, R., Qiao-Grider, Y., & Hung, L.-F. (2005). Peripheral vision can influence eye growth and refractive development in infant monkeys. *Investigative Ophthalmology and Vision Science, 46*, 3965–3972.

Thibos, L. N. (2002). Are higher order wavefront aberrations a moving target unworthy of clinical treatment? *Journal of Refractive Surgery, 18*, 744–745.

Thibos, L. N., Applegate, R. A., Schwiegerling, J. T., & Webb, R. (2002a). Standards for reporting the optical aberrations of eyes. *Journal of Refractive Surgery, 18*, S652–S660.

Thibos, L. N., Hong, X., Bradley, A., & Cheng, X. (2002b). Statistical variation of aberration structure and image quality in a normal

population of healthy eyes. *Journal of Optical Society of America A, Optics, Images, Science, and Vision, 19*, 2329–2348.

Troilo, D., & Wallman, J. (1991). The regulation of eye growth and refractive state: An experimental study of emmetropization. *Vision Research, 31*, 1237–1250.

Wallman, J., & Winawer, J. (2004). Homeostasis of eye growth and the question of myopia. *Neuron, 43*, 447–468.

Walsh, G., & Charman, W. N. (1985). Measurement of the axial wavefront aberration of the human eye. *Ophthalmic and Physiological Optics, 5*, 23–31.

Wang, B., & Ciuffreda, K. J. (2006). Depth-of-focus of the human eye: Theory and clinical implications. *Survey of Ophthalmology, 51*, 75–85.

Wildsoet, C. F. (1997). Active emmetropization—Evidence for its existence and ramifications for clinical practice. *Ophthalmic and Physiological Optics, 17*, 279–290.

Wildsoet, C. F., & Schmid, K. L. (2000). Optical correction of form deprivation myopia inhibits refractive recovery in chick eyes with intact or sectioned optic nerves. *Vision Research, 40*, 3273–3282.

Wilson, B. J., Decker, K. E., & Roorda, A. (2002). Monochromatic aberrations provide an odd-error cue to focus direction. *Journal of Optical Society of America A, Optics, Images, Science, and Vision, 19*, 833–839.

Winawer, J., & Wallman, J. (2002). Temporal constraints on lens compensation in chicks. *Vision Research, 42*, 2651–2668.